Mobility of Bodies in Contact—Part II: How Forces are Generated by Curvature Effects

Elon Rimon and Joel W. Burdick

***Abstract*— This paper considers how forces are produced by compliance and surface curvature effects in systems where an object $\mathcal{B}$ is kinematically immobilized to second-order by finger bodies $\mathcal{A}_1, \cdots, \mathcal{A}_k$. A class of configuration-space based elastic deformation models is introduced. Using these elastic deformation models, it is shown that any object which is kinematically immobilized to first or second-order is also dynamically locally asymptotically stable with respect to perturbations. Moreover, it is shown that for preloaded grasps kinematic immobility implies that the stiffness matrix of the grasp is positive definite. The stability result provides physical justification for using second-order effects for purposes of immobilization in practical applications. Simulations illustrate the concepts.**

***Index Terms*—Compliance modeling, configuration space, contact, dynamics, fixturing, geometry, grasping, kinematics, stability.**

I. Introduction

In [22], we introduced a configuration-space based method for analyzing the mobility of an object $\mathcal{B}$, held with frictionless contact by k finger bodies $\mathcal{A}_1, \cdots, \mathcal{A}_k$ in an equilibrium grasp. In our approach, the ith-order mobility of $\mathcal{B}$ is derived from the ith-order properties of the *free motion* curves of $\mathcal{B}$ in its configuration space. The first-order properties of these curves lead to a first-order mobility theory which is equivalent to classical mobility theories based on the instantaneous notions of forces and velocities. We showed that first-order mobility theories are often too crude in practice. This motivated our development of a novel second-order mobility theory. The combined first- and second-order theories determine the mobility of $\mathcal{B}$ in all generic equilibrium grasps.

While the second-order mobility theory is kinematic in nature, its potential applications (several of which are mentioned in the discussion section) rely upon contact forces generated by surface curvature effects. For example, in *fixture planning* the goal is to design fixtures that completely restrain a given class of objects. From the configuration-space (c-space) perspective, the goal is to completely isolate an object's contact configuration from the remainder of its freespace, where the fixtures determine the c-space obstacles. The minimal three-finger grasp of Fig. 8, for instance, can be regarded as a work holding problem. As discussed in [22], the object has a vanishing 2nd-order mobility index in this example, and is therefore completely immobilized. However, this immobilization cannot be fully explained in terms of forces at the contact points, since conventional force-closure theory would dictate that 4 forces are needed to counterbalance any applied external wrench. Thus, our goal is to study the nature of the restraining forces generated by second-order immobilization and the stability of grasps or fixture arrangements that rely upon such effects.

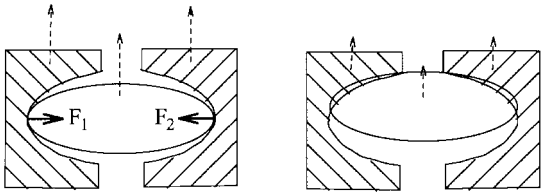

Fig. 1. (a) The fingers and object move with uniform velocity. (b) Once the fingers slow down the object must penetrate the fingers.

An *ideal rigid body model* allows no deformation or interpenetration to occur when two bodies are pressed into contact. The following paradox [5], [14], which is analyzed in more depth in [20], illustrates that contact forces generated by second-order effects cannot be completely explained within the context of ideal rigid body models. Let $\mathcal{B}$ be an ellipse, held along its major axis by two concave fingers, as shown in Fig. 1(a). It can be verified that $\mathcal{B}$ is immobilized to second-order by the fingers. The fingers push on $\mathcal{B}$ with equal and opposite forces, $F_1 = -F_2$, so that the net wrench on $\mathcal{B}$ is zero (i.e., an equilibrium grasp). At time $t < 0$ the three bodies travel upward with constant velocity. At time $t = 0$ the fingers begin to slow down, attempting to bring $\mathcal{B}$ to a halt, while maintaining their upward motion, without rotating or sliding sideways. It follows from the ideal rigid body assumption that $\mathcal{B}$ must be slowing down with the fingers. However, the rigid body assumption only allows each finger to apply a force normal to the object's boundary, and therefore it is impossible to slow down the body. But practical experience indicates that $\mathcal{B}$ does slow down with the fingers. Hence it must be that the contact forces shift their direction with respect to the upward direction at time $t = 0$. Within a strictly rigid-body model no such shift is possible, as this would require interpenetration of the bodies as illustrated in Fig. 1(b). Additional assumptions must be added to the contact model in order to fully explain the dynamics associated with second-order immobilization.

Manuscript received September 28, 1994; revised June 20, 1997. This paper was supported by the Office of Naval Research Young Investigator Award N00014-92-J-1920.This paper was recommended for publication by Associate Editor Y. Nakamura and Editor A. Goldenberg upon evaluation of the reviewers' comments.

E. Rimon is with the Department of Mechanical Engineering, Technion, Israel Institute of Technology, Haifa 32000, Israel.

J. W. Burdick is with the Department of Mechanical Engineering, California Institute of Technology, Pasadena, CA 91125 USA.

Publisher Item Identifier S 1042-296X(98)07320-0.

To analyze the forces generated by second-order effects, we introduce a class of lumped-parameter elastic deformation models. Our focus on elastic contact models is motivated by the important role that elastic deformation plays in fixture planning and grasp stability. These models, which are motivated by the work of Gesley [7], capture the qualitative behavior of the elastic deformation of contacting bodies, without the need to compute the explicit distribution of the surface deformation at the contacts (such as in [23]). These models are nonlinear and admit a configuration-space based representation. The class of models also includes the well known and widely used Hertz contact model [9]. We use these models because the linear spring models commonly used in grasp and fixture analysis are *not* supported by experiments or by solid mechanics theory [12], [13]. The establishment of the basic properties of these compliance models is another contribution of this paper.

While these configuration-space based contact models are useful in their own right, our principal goal is to use these models to investigate the dynamic stability of objects which are immobilized according to our kinematic theory. Using these models, we prove that *if an elastic object is kinematically immobilized to first or second-order (as determined by the coordinate invariant 1st and 2nd-order mobility indices), its contact configuration with zero velocity is dynamically locally asymptotically stable*. That is, when $\mathcal{B}$ is perturbed, the forces generated by elastic deformation at the contacts bring $\mathcal{B}$ back to its original configuration. In other words, the grasp is passively stable. As a corollary, it is true that the stiffness matrix associated with any kinematically immobilizing preloaded grasp is positive definite. Furthermore, the stability result holds for any model in our broad class of elastic deformation models, including the Hertz contact model.

In the related literature, Baraff [1] used elastic deformation to model the dynamics of contacting bodies. However, he focuses on dynamically evolving systems of bodies while we focus on grasping and the stability of grasps. Other authors have considered elastic deformation in grasping. For example, Hanafusa and Asada [8] implemented an elastic-rods mechanism capable of stably grasping objects based on a mixture of what we would call first and second-order ideas. Their work was subsequently extended by Nguyen [18], who showed using a linear spring model that an object which is first-order immobile is also passively stable. Cutkosky and Kao [4], and Montana [16], [17], analyzed the stability of grasps under small perturbation of the contacting fingers. Our work develops a more complete stability result for a much broader and more sophisticated range of modeling assumptions than have previously appeared in the literature. Further, we prove the stability of systems which are second-order immobile, a heretofore novel idea which has important potential applications in grasp, posture, and fixture planning.

Recent work by Howard and Kumar [10] on stability of multiple-finger grasps also allows for small elastic deformations. They derive related stability results using a different approach. While their work assumes a linear spring deformation model, we consider a general class of nonlinear c-space based deformation models which includes the Hertz model. They use the grasp's stiffness matrix to determine stability, which requires that no object-finger contact be broken during the perturbation of the object about its equilibrium grasp. Our stability criterion holds for all object perturbations, including those where contacts are broken. Moreover, for preloaded grasps our stability test becomes a positive-definiteness criterion of a generalized stiffness matrix. In a work published after this paper was submitted, Ponce [19] applied our second-order mobility theory to the immobilization of polyhedral objects. Using four elastic rods, he showed that second-order immobile grasps are automatically stable. Ponce's result relies on the flatness of the polyhedral faces and it holds for one type of fingers or fixtures. However, it corroborates the completely general stability result described in this paper.

The paper is organized as follows. A class of lumped-parameter elastic deformation models is introduced in Section II. Section III is devoted to the proof of dynamic stability for objects which are kinematically immobilized. Section IV provides an extension of the stability result to loaded grasps. Section V presents simulations to verify the models and theory of Sections II and III. Finally, Section VI considers possible applications of our 2nd-order mobility theory. We use the notation and concepts of the companion paper [22].

II. Elastic Deformation Contact Models

We now introduce a class of lumped parameter *elastic deformation contact models* that relate the contact force between two bodies to their relative displacement. In these models we are not concerned with the details of the surface deformation. Rather, we only require the model to provide a relationship between the contact force and the displacement of reference frames fixed on the contacting bodies. This is the "lumped parameter" aspect of our models. We first consider a simple model proposed by Gesley [7], then extend the model to a more general class of elastic contact models, which includes the well known and well justified Hertzian contact model.

A. Gesley's Model

In Gesley's model for computing the interaction forces due to elastic deformation, the bodies are considered to be rigid. When two bodies are pressed together, imagine that the rigid body shapes could freely interpenetrate without deformation during a relative approach, so that their volumes are allowed to overlap in the vicinity of the contacts. The overlap approximately models the act of interbody deformation. Similarly, it is postulated that the overlap gives rise to a force which approximates the interbody forces. Gesley's model circumvents the need to compute the distribution of the contacting bodies' surface deformations. Moreover, the model is known to predict the behavior of mechanisms involving small deformations, such as a clock mechanism [7]. On the other hand, the model applies only to quasi-rigid objects, whose deformation is confined to the vicinity of the contacts. We now pursue a more formal development of the overlap model, which did not appear in Gesley's work.

Recall that $\mathcal{A}_i$ is assumed stationary, and that $\mathcal{B}(q)$ is the set occupied by $\mathcal{B}$ when it is at a configuration q. Recall, too, that $\mathcal{CA}_i$ is the c-obstacle associated with $\mathcal{A}_i$ and $\mathcal{S}_i$ is its

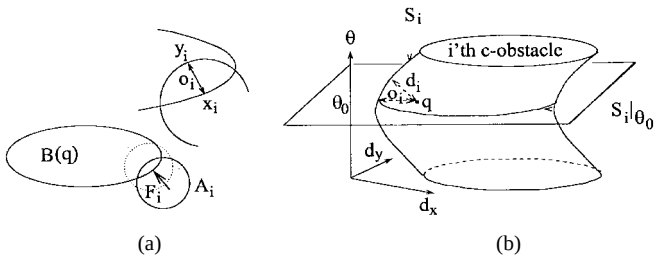

Fig. 2. (a) The overlap o_i. (b) C-space interpretation of o_i.

boundary. The *overlap* between $\mathcal{B}(q)$ and $\mathcal{A}_i$ is described by the *overlap function* $o_i(q)$. It is defined as the minimal amount of translation of $\mathcal{B}$ required to separate it from $\mathcal{A}_i$ [Fig. 2(a)]. The amount of overlap at a configuration $q_0 = (d_0, \theta_0)$ is obtained by minimizing $\|d - d_0\|$ over all translations d such that $\mathcal{B}(d, \theta_0)$ and $\mathcal{A}_i$ touch each other while their interiors are disjoint. These configurations (d, θ_0) are points in the intersection of $\mathcal{S}_i$ with a hyperplane of configurations (d, θ) with $\theta = \theta_0$. Let $\mathcal{S}_i|_{\theta_0}$ denote this set. Then o_i can be interpreted as a generalized distance in c-space

$$o_i(d,\theta) = \begin{cases} \mathsf{dst}(d, \mathcal{S}_i|_\theta), & \text{if } q \text{ is inside } \mathcal{CA}_i \\ 0, & \text{if } q \text{ is outside } \mathcal{CA}_i. \end{cases} \tag{1}$$

Note that o_i is similar to d_i, the signed Euclidean distance from $\mathcal{S}_i$ introduced in [22], except that o_i is positive inside $\mathcal{CA}_i$ and identically zero outside it [Fig. 2(b)]. However, note that o_i is *nonsmooth* on $\mathcal{S}_i$.

Let x_i be the point on the surface of $\mathcal{B}(q)$ and let y_i be the point on the surface of $\mathcal{A}_i$ which correspond to the maximum penetration of the two bodies [Fig. 2(a)]. Using this notation, the minimum translation of $\mathcal{B}$ that separates it from $\mathcal{A}_i$ occurs along the line segment $\overline{x_i y_i}$, and $o_i = \|y_i - x_i\|$. The force *action point* is set to x_i, and its *direction* is taken as $y_i - x_i$, pointing into $\mathcal{B}$ [Fig. 2(a)]. That is, the distribution of interbody forces which arise from elastic deformation at the contact is approximated by a single force acting at x_i in the direction $y_i - x_i$. Let $F_i(x_i)$ denote this force. Then the model postulates that the *magnitude* of F_i depends on o_i as follows:

$$\|F_i(x_i)\| = \begin{cases} \eta_i o_i & \text{if } o_i > 0 \\ 0 & \text{if } o_i = 0 \end{cases} \quad \text{where } \eta_i > 0. \tag{2}$$

This model basically consists of a spring with a spring constant η_i. However, note that *this is NOT necessarily a linear spring model*, since o_i usually does not vary linearly with respect to the displacement q of $\mathcal{B}$. Unlike the simplified and ad-hoc linear spring models used by many previous investigators, this model more faithfully takes the object's geometry into account when computing the effective contact compliance. Gesley's model also includes a damping term proportional to o_i and $\dot{o}_i$. We discuss and generalize this damping term in [20].

Next we describe several important properties of the contact model, not considered by Gesley. The following lemma asserts that F_i is perpendicular to the surfaces of $\mathcal{B}$ and $\mathcal{A}_i$.

Lemma 2.1 [20]: Let $\mathcal{B}(q)$ overlap $\mathcal{A}_i$. Then the overlap segment $\overline{x_i y_i}$ is **perpendicular** to the surface tangents of $\mathcal{B}(q)$ and $\mathcal{A}_i$ at the respective endpoints.

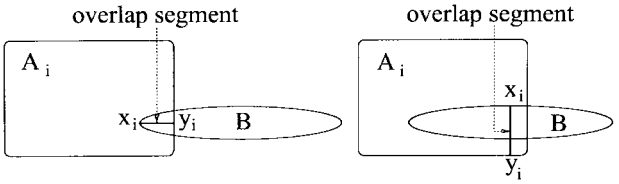

Fig. 3. The overlap segment lies in $\mathcal{B} \bigcap \mathcal{A}_i$ for small overlaps, but not for deep ones.

We may now express the force F_i in terms of the inward pointing unit normal to the surface of $\mathcal{B}$ at x_i, denoted $\hat{N}(x_i)$, as follows:

$$F_i(x_i) = \begin{cases} \eta_i o_i \hat{N}(x_i) & \text{if } o_i > 0 \\ 0 & \text{if } o_i = 0. \end{cases} \tag{3}$$

For the model to be viable, the overlap segment must lie in the intersection of $\mathcal{B}(q)$ and $\mathcal{A}_i$. This is addressed in the following lemma.

Lemma 2.2: For all sufficiently small values of $o_i(q)$, the overlap segment $\overline{x_i y_i}$ lies wholly inside the intersection set $\mathcal{B}(q) \bigcap \mathcal{A}_i$.

The lemma follows from the interpretation of $o_i(d, \theta)$ as $\mathsf{dst}(d, \mathcal{S}_i|_\theta)$. Fig. 3 shows that the overlap segment may cease to lie in the intersection set for "deep" overlaps. Of course, physically plausible interpenetrations are always very small. For instance, in bodies made of steel these overlaps rarely exceed tens of microns (see Section V). The following proposition, whose proof appears in the appendix, specifies the c-space wrench generated by $F_i(x_i)$.

Proposition 2.3: Let $\mathcal{A}_i$ be stationary and let $\mathcal{B}(q)$ have overlap $o_i(q) > 0$ with $\mathcal{A}_i$. Any interbody force $F(x_i)$ acting on $\mathcal{B}$ along the overlap segment $\overline{x_i y_i}$ into $\mathcal{B}$ gives a **wrench**

$$w(q, F_i) = -\|F_i\| \nabla o_i(q).$$

In particular, the **wrench** due to the contact force $F_i(x_i)$ of Gesley's model is

$$w(q, F_i) = \begin{cases} -\eta_i o_i(q) \nabla o_i(q) & \text{if } o_i(q) > 0 \\ 0 & \text{if } o_i(q) = 0. \end{cases} \tag{4}$$

It can be verified that the wrench in (4) is Lipschitz continuous with respect to q.

The Hertz Contact model: A more traditional lumped-parameter elastic contact model, which has been corroborated in experiments and is consistent with solid mechanics theory, is due to Hertz [9]. Hertz postulated a specific interbody force distribution, whose integration according to the principals of linear elasticity yields an expression for the net deformation at every surface point. This expression can be used to develop the lumped parameter relationship that we need. Let two frames be attached to each of the contacting bodies, where it is assumed that the frames are sufficiently "far" from the deforming contact region. When the two bodies are pressed together by a force P along their contact normal, the two frames approach each other by a distance δ. The relation between δ and the magnitude of P is given by $\delta = \frac{1}{c}\|P\|^{2/3}$, where c is a positive constant which depends on the elasticity of the bodies and their undeformed contact geometry [9]. For a contact of $\mathcal{B}$ with $\mathcal{A}_i$, it can be shown that δ is exactly the

overlap o_i, and c is related to the spring constant η_i. Thus, the contact force according Hertz is

$$F_i(x_i) = \begin{cases} (\eta_i o_i^{3/2})\hat{N}(x_i) & \text{if } o_i > 0 \\ 0 & \text{if } o_i = 0. \end{cases} \quad (5)$$

Hertz's theory provides an expression for the spring constant η_i in terms of the bodies' material properties and contact geometry. Otherwise, it is remarkably similar to Gesley's naive formula. References [12] and [13] more fully exploe the modeling of Hertzian contact via overlap functions.

A general class of contact models: The spring force of both models gives rise to a wrench. Proposition 2.3 implies that this wrench is the negated gradient of the following elastic potential energy function:

$$U_i(q) = \frac{1}{2+p}\eta_i o_i^{2+p}(q) \quad (6)$$

where $p = 0$ in Gesley's model and $p = 0.5$ in Hertz's model. More generally, the ensuing stability result holds for any elastic contact model in which $U_i(q)$, corresponding to contact of $\mathcal{B}(q)$ with $\mathcal{A}_i$, satisfies the following two requirements. First, U_i must be strictly positive inside $\mathcal{CA}_i$ and zero on the boundary $\mathcal{S}_i$. This implies that the interbody force should increase with increasing deformation. Unless tensile forces are realizable (i.e., the surface is "sticky"), $U_i(q)$ should be zero outside $\mathcal{CA}_i$. Second, U_i must be differentiable, such that ∇U_i is Lipschitz continuous. As we shall see, the crucial property of these potentials is that when $\mathcal{B}(q_0)$ is kinematically immobilized by k elastic bodies, q_0 becomes a strict local minimum of the potential function $U(q) = \sum_{i=1}^{k} U_i(q)$.

III. Stability of Kinematically Immobile Objects

The introduction of the elastic contact model was necessitated by the failure of the rigid-body idealization to explain how restraint forces are generated by second-order effects. We consider in this section the predictive powers of our kinematic mobility theory when applied to the dynamic stability of bodies satisfying the elastic contact model. We show that kinematic immobility guarantees dynamic stability when elastic deformation effects are taken into account. That is, if $\mathcal{B}$ is immobilized, and a perturbing force is applied to $\mathcal{B}$, it will return to its equilibrium grasp configuration once the perturbation is removed. While this result meets with intuition, this work contains the most general proof of this fact, and proves it for the previously unconsidered case of second-order immobility. The result also justifies using second-order effects in applications, as discussed in the concluding section.

First recall the definition of kinematic immobility from [22], which is based on the 1st and 2nd-order mobility indices.

Definition 1: An object $\mathcal{B}$ held in equilibrium grasp by k fingers is **completely immobile** if its configuration q_0 is isolated from the remainder of its freespace by the fingers' c-obstacles. $\mathcal{B}$ is **immobile to first order** if $m^1_{q_0} = 0$, and is **immobile to second order** if $m^2_{q_0} = 0$.

From the definitions of $m^1_{q_0}$ and $m^2_{q_0}$ it follows that ith order immobility suffices for complete immobility, for $i = 1,2$. Moreover, *curvature effects can lower effective mobility*, since $0 \le m^2_{q_0} \le m^1_{q_0}$. That is, a grasp which does not immobilize $\mathcal{B}$ to first order may actually immobilize it when second-order effects are taken into account.

Theorem 1 below relates kinematic immobility to the forces of restraint, and is a major contribution of this paper. In the theorem, we make the following assumptions. We assume that $\mathcal{B}$ is initially contacted by k undeformed fingers, such that the fingers maintain point contact with $\mathcal{B}$. Once $\mathcal{B}$ is perturbed from equilibrium, its dynamics are determined by wrenches resulting from the fingers' elastic deformation forces, $F_i(x_i)$ for $i = 1, \cdots, k$, and by wrenches resulting from damping. The damping is caused by inelastic material compression effects and possibly surface friction. For the sake of brevity, we lump the damping effects at the ith contact into a single vector field $\xi_i o_i(q) g_i(q, \dot{q})$, such that $\xi_i > 0$ is a damping coefficient, $o_i(q)$ is the overlap function, and $g_i(q, \dot{q})$ is a smoothly varying dissipative vector field. Technically, $g_i(q, \dot{q})$ is a dissipative vector field if it satisfies $g_i(q, \dot{q}) \cdot \dot{q} < 0$ along trajectories of the mechanical system. In [20], we develop a more detailed damping model that is consistent with tribological models and experimental studies. To summarize, the corresponding Lagrangian dynamics of $\mathcal{B}$ is

$$\frac{d}{dt} D_{\dot{q}} K(q, \dot{q}) - D_q K(q, \dot{q}) = \sum_{i=1}^{k} \begin{cases} -o_i(\eta_i \nabla o_i(q) + \xi_i g_i(q, \dot{q})) & o_i(q) > 0 \\ 0 & o_i(q) = 0 \end{cases} \quad (7)$$

where $K(q, \dot{q})$ is the kinetic energy of $\mathcal{B}$, and the contact forces arise from Gesley's model. The vector-field on the right is Lipschitz continuous, which implies the existence and uniqueness of solutions to (7). We may now state the theorem.

Theorem 1: Let $\mathcal{B}$ be at a configuration q_0, in contact with k disjoint fingers which are positioned around $\mathcal{B}$ in an essential equilibrium grasp arrangement. Let the object and fingers satisfy Gesley's elastic contact model (4), such that none of the contacting bodies is initially deformed. If $\mathcal{B}$ is (kinematically) **immobilized to first or second order**, its zero velocity state $(q_0, 0)$ is (dynamically) **locally asymptotically stable**.

Before proving the theorem we consider its physical interpretation. The theorem states that if a small perturbing force is applied to $\mathcal{B}$ while $\mathcal{B}$ is immobilized to first or second order, then when the perturbing force is removed, $\mathcal{B}$ is guaranteed to stabilize to its equilibrium grasp configuration with zero velocity. In particular, the ellipse paradox depicted in Fig. 1 can now be explained in terms of temporary deformation of the decelerating fingers as to generate forces opposing the motion of $\mathcal{B}$. The theorem guarantees that the object/fingers system will settle to its original, undeformed, position.

Proof: To prove the theorem, we need the following fact concerning the stability of damped mechanical systems under the influence of potential fields. A Lagrangian mechanical system of the form

$$\frac{d}{dt}\frac{\partial}{\partial \dot{q}} K - \frac{\partial}{\partial q} K = w \quad (8)$$

is a *damped mechanical system*[1] when $w(t)$ is of the form

[1] It is more accurately a *damped mechanical system governed by a potential energy function.*

$w(t) = -\nabla U(q) + w_d(q, \dot{q})$, where $U(q)$ is a potential energy function and $w_d(q, \dot{q})$ is a dissipative vector field. The stability result, attributed to Kelvin [11], [24], is *the local minima of U, with zero velocity, of a damped mechanical system are local attractors of its flow*.

For Gesley's compliance model, it is shown in Corollary A.4 that $\nabla(\frac{1}{2}o_i^2) = o_i \nabla o_i$. Hence $\mathcal{B}$ in the dynamical equation (7) is subjected to a potential energy $U(q) = \sum_{i=1}^{k} \frac{1}{2}\eta_i o_i^2(q)$.

To use Kelvin's result, we must establish that the equilibrium configuration is a strict local minimum of the elastic potential $U(q)$. The function $U(q)$ vanishes at q_0, since $o_i(q_0) = 0$ for $i = 1, \cdots, k$. Let $q(t)$ be a smooth c-space path such that $q(0) = q_0$, and recall that $d_i(q)$ is the signed distance of q from $\mathcal{S}_i$. By definition of first-order immobility, the first-order approximation to $q(t)$ penetrates one of the finger c-obstacles. Hence $\frac{d}{dt}|_{t=0} d_i(q(t)) < 0$ for some $1 \leq i \leq k$. Similarly, by definition of second-order immobility, the second-order approximation to $q(t)$ penetrates one of the c-obstacles. This implies that either $\frac{d}{dt}|_{t=0} d_i(q(t)) < 0$ for some $1 \leq i \leq k$, or $\frac{d}{dt}|_{t=0} d_j(q(t)) = 0$ for $j = 1, \cdots, k$ and then $\frac{d^2}{dt^2}|_{t=0} d_i(q(t)) < 0$ for some $1 \leq i \leq k$. Hence, if $\mathcal{B}$ moves from its equilibrium configuration along a trajectory $q(t)$, at least one d_i becomes negative after $t = 0$. This implies that at least one o_i becomes positive after $t = 0$. Thus $U(q(t))$ is locally increasing along any $q(t)$, and q_0 is a strict local minimum of U. This establishes the requirement of Kelvin's stability result, and $(q_0, 0)$ is locally asymptotically stable. □

The stability result can be extended to *any* elastic deformation model of the form (6). This is stated in a more general form in the following corollary. Recall that $\mathcal{CA}_i$ denotes the c-obstacle corresponding to the finger $\mathcal{A}_i$.

Corollary 3.1 Theorem 1 applies to any elastic potential energy function $U(q) = \sum_{i=1}^{k} U_i(q)$, where each U_i is positive inside $\mathcal{CA}_i$, zero outside it, and is differentiable with Lipschitz continuous derivative. In particular, the theorem applies to any elastic potential of the form (6), which includes the classical Hertz model.

To reiterate, the theorem and its corollary state that if $\mathcal{B}$ is kinematically immobilized to first or second order, and if $\mathcal{B}$ and $\mathcal{A}_1, \cdots, \mathcal{A}_k$ satisfy any of the aforementioned elastic deformation models, then $\mathcal{B}$ will be asymptotically stable with respect to small perturbations. In the first-order context, the result implies that if the fingers are arranged in a frictionless force closure arrangement (which is equivalent to first-order immobility), then $\mathcal{B}$ is *passively* stable due to compliance effects. Similarly, if $\mathcal{B}$ is immobilized to second order (which may use fewer fingers than required for frictionless force closure [22]), it is also *passively* stable. The kinematic notion of second-order immobility ensures that small perturbations will deform the contacts so as to provide the appropriate restoring forces that bring $\mathcal{B}$ back to equilibrium.

IV. The Stability of "Loaded" Grasps

In Theorem 1 we assume that the contacting bodies are initially undeformed. However, this assumption is not always justified in practical applications. For example, in fixturing applications the fingers or fixtures typically apply nonzero initial forces to the grasped object, which cause initial deformation of the contacting bodies. The following theorem asserts that the stability of the undeformed contact arrangement is preserved by loaded grasps which are sufficiently close to it.

Theorem 2: Let $\mathcal{B}$ be immobilized to first or second-order by k fingers as described in Theorem 1. Then there exist positive upper bounds $o_{1,\max}, \cdots, o_{k,\max}$ such that all equilibrium grasps obtained by pressing the fingers along the contact normals such that $o_i \in (0, o_{i,\max}]$ for $i = 1, \cdots, k$, are **locally asymptotically stable**.

In particular, the **stiffness matrix**[2] of any of the above loaded grasps is **positive definite**.

In other words, we start with an "unloaded" equilibrium arrangement, then press the fingers against $\mathcal{B}$ along the respective contact normals. The theorem guarantees that the stability of the unloaded grasp is preserved by the loaded grasps, provided that the overlaps with $\mathcal{B}$ are smaller than $o_{i,\max}$. The assumption that the o_i's are small is reasonable, since in most real grasps (or fixture states) the contacting fingers start in an unloaded equilibrium state, then slowly increase their contact force until the final loaded state is reached. From a technical perspective, the assumption on the loading process is required in order to make a connection between our concept of immobility, which is defined for unloaded states, and stability of a loaded grasp. The proof of the theorem appears in [20]. Here we merely give a sketch of the proof.

Sketch of Proof: The elastic potential energy function, $U(q) = \sum_{i=1}^{k} \frac{1}{2}\eta_i o_i^2(q)$, is locally smooth for any of the loaded grasps. According to Kelvin's stability result, local asymptotic stability is guaranteed if U has a local minimum at q_0. To show this, it suffices to show that the grasp *stiffness matrix*, $D^2U(q_0)$, is positive definite i.e., that $\dot{q}^T D^2U(q_0)\dot{q} > 0$ for all $\dot{q} \in T_{q_0}\mathbb{R}^m$. Thus consider $D^2U(q_0)$

$$D^2U(q_0) = \sum_{i=1}^{k} \eta_i \nabla o_i(q_0) \nabla o_i(q_0)^T + \sum_{i=1}^{k} \eta_i o_i(q_0) D^2 o_i(q_0). \tag{9}$$

In the case of first-order immobility, the c-obstacle normals $\hat{n}_1(q_0), \cdots, \hat{n}_k(q_0)$ span the entire ambient tangent space $T_{q_0}\mathbb{R}^m$. We show that $\nabla o_i(q_0)$ is collinear with $\hat{n}_i(q_0)$ for $i = 1, \cdots, k$, and consequently the matrix $\sum_{i=1}^{k} \eta_i \nabla o_i(q_0) \nabla o_i(q_0)^T$ is positive definite. It follows from (9) that $D^2U(q_0)$ is positive definite for all sufficiently small overlaps $o_i(q_0)$. In the case of second-order immobility, the c-space relative curvature form, $\kappa_{\text{rel}}(q_0, \dot{q})$, is related to the second-derivatives of the overlap functions as follows:

$$\sum_{i=1}^{k} \eta_i o_i(q_0) \dot{q}^T D^2 o_i(q_0) \dot{q} = -\left(\sum_{i=1}^{k} \eta_i o_i(q_0) \|\nabla o_i(q_0)\| \right) \kappa_{\text{rel}}(q_0, \dot{q}). \tag{10}$$

Let V_1 be the subspace of $T_{q_0}\mathbb{R}^m$ spanned by the vectors $\hat{n}_1(q_0), \cdots, \hat{n}_k(q_0)$, and let V_2 be its orthogonal complement. By definition of second-order immobility, $\kappa_{\text{rel}}(q_0, \dot{q}) < 0$ for

[2] I.e., the second-derivative or Hessian matrix of the elastic potential energy.

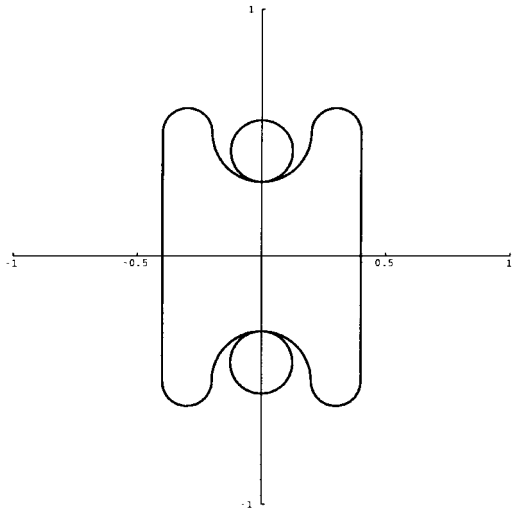

Fig. 4. Two-finger planar grasp which is 2nd-order immobile, but has 1st-order mobility of 2.

all $\dot{q} \in V_2$. Since $o_i(q_0) > 0$ for loaded grasps, the right side of (10) is positive for all $\dot{q} \in V_2$. Thus, while the matrix $\sum_{i=1}^{k} \eta_i \nabla o_i(q_0) \nabla o_i(q_0)^T$ takes care of the positive definiteness on V_1, $\kappa_{\text{rel}}(q_0, \dot{q})$ contributes to it on V_2. The details of how the positive definiteness propagates to the entire space $T_{q_0}I\!R^m$ are given in [20]. □

It should be observed that the stiffness matrix in (9) depends on the overlap functions and their derivatives. Thus, the choice of contact model can influence the determination of stability. Since linear-spring models are not supported by experiments or results from elasticity theory, it is hard to justify their use for stability analysis. In particular, linear-spring models can lead to erroneous conclusions about the magnitude of the influence of second-order effects on compliant stability. In contrast, the overlap function implementation of the Hertz model provide a more reliable measure for grasp stiffness [12].

V. Simulations

In this section, we briefly present the results of simulations which illustrate the theory described above. We first consider a planar object grasped by two disc fingers, as shown in Fig. 4. The 1st-order mobility index of this grasp is $m^1_{q_0} = 2$. However, because of the concavity at the contact points, the object is immobilized to second order. Thus, second order effects play an important role in this example.

We assume that the object is made of homogeneous material, and therefore its center of mass is located at its geometric center. The object's reference frame is fixed at this center of symmetry. Further, we assume the Gesley elastic deformation model, with damping of the form $-\xi_i o_i(q)\dot{q}$. That is, we implement the dynamics of (7). Other elastic deformation models lead to analogous results.

We assume that the object is made from a 1 cm thick slab of steel, with maximum dimension from top-to-bottom of 12 cm and width of 8 cm. The radius of the "dimples" in the object is 2.0 cm, while the other radii are 1.0 cm. Assuming that steel has a density of 7,830 kg/m^3, the mass of this object is 0.577 kg, and its moment of inertia about the center of mass is $0.000\,858$ kg $\cdot$ m^2. The fixtures are circular, with radius of 1 cm. The spring constant is $\eta = 8.74 \times 10^{10}$ N/m—which is the spring constant calculated by the Hertz contact model. The damping constant, ξ, is $(1/1.2)\eta$, a number obtained from experiments on curved steel bodies [6]. Practically speaking, this example corresponds to a realistic fixturing problem.

Fig. 5(a) shows the time history of the y coordinates of $\mathcal{B}$'s reference frame for a situation in which the object is perturbed by 10 μm in the y direction, and then released at $t = 0$. The response of the x and θ coordinates is negligible and is not shown. As seen in the simulation, the object does indeed converge back to the equilibrium state, which is located at $(x, y, \theta) = (0, 0, 0)$. Similarly, Fig. 5(b) shows the time history of the object's x-coordinate for the case in which the body is displaced by 10 μm in the x direction, and then released at $t = 0$ (the time histories of the other coordinates show no meaningful information). Fig. 6 shows time history of all coordinates when the body is displaced by 0.004 rad in the θ direction, and then released at $t = 0$.

A second set of simulations was performed for a triangular object grasped by three disc fingers (or fixtures), shown in Fig. 8(b). The object is circumscribed by an equilateral triangle whose sides have length 10 cm. The finger radii are 1 cm. We assume that the object and fingers are comprised of steel, having a 1 cm thickness. The object mass is 0.339 kg, while its inertia is $0.000\,141$ kg $\cdot$ m^2. We use the same spring and damping constants as the previous example.

Fig. 7(a) shows the object's y-coordinate versus time for the case in which the body is displaced by 10 μm in the y direction, and then released at $t = 0$ (the time histories of the other coordinates show no meaningful information). That is, the object is perturbed in a direction which is a penetration motion to first order. Fig. 7(b) shows the object's θ-coordinate versus time for the case in which the body is displaced by 0.004 rad in the θ direction, and then released at $t = 0$. In this case the perturbation occurs along a motion which is free to first order, but a penetration motion to second order.

In summary, the simulations validate the stability predicted by Theorem 1. Second-order effects do indeed immobilize objects which are mobile to first order. The dynamic response differs when the object is perturbed in directions which correspond to 1st-order free motions, as opposed to perturbations in directions which are 1st-order penetration motions. Generally, it takes the object longer to return to equilibrium when perturbed along 1st-order free motions, since the stability is provided solely by 2nd-order effects. In a sequel to this paper [12], we further study the restraining forces generated by first and second order effects. These studies show that restraining forces due to 2nd-order effects can be made comparable in magnitude to 1st-order forces when the object is grasped at concavities, or when the object is grasped by concave fingers. See [12] for more details.

VI. Conclusion

In [22], we considered the issue of immobilization in a geometric setting and introduced the new concept of second-order immobility. In this paper we investigated the compliant

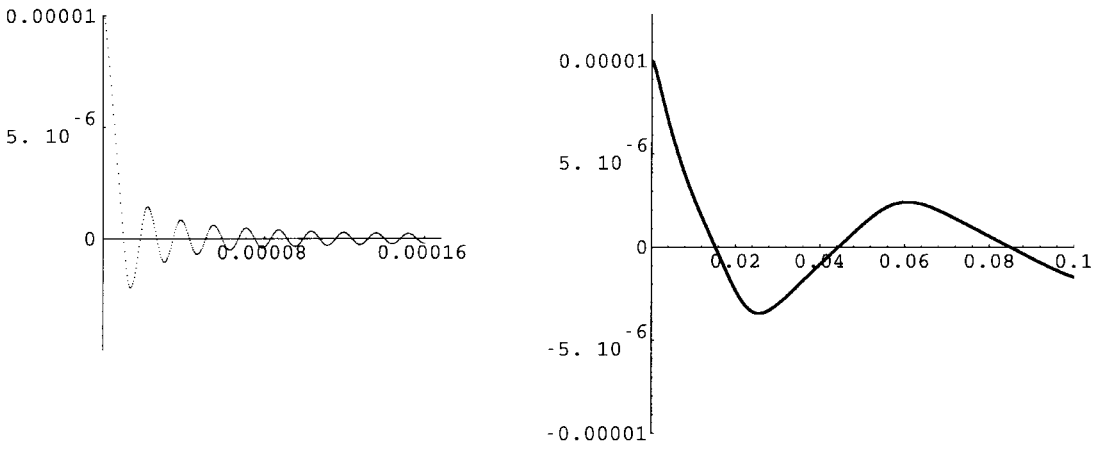

(a) (b)

Fig. 5. (a) y (in meters) versus time (in seconds) for the two-finger grasp, when the object is perturbed in the y direction and (b) x (in meters) for the two-finger grasp, when the object is perturbed in the x direction.

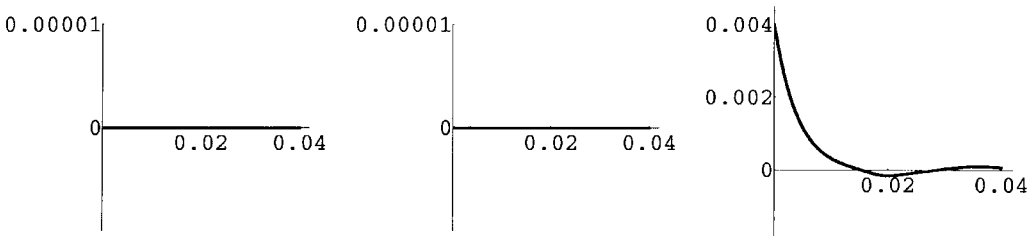

Fig. 6. x (in meters), y (in meters), and θ (in radians) versus time (in seconds) for the two-fingered grasp, when the object is perturbed in the θ direction.

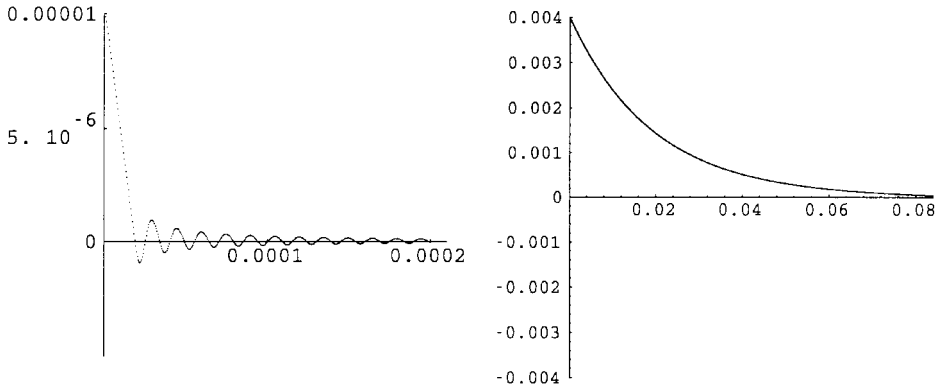

Fig. 7. y (in meters) versus time (in seconds) for the three-finger grasp, when the triangular object is perturbed: (a) in the y-direction and (b) in the θ-direction.

stability of grasps that are deemed immobile by geometric analysis based on a rigid body simplification. We showed that first and second-order immobilization is equivalent to compliant stability for a broad range of compliant contact models. This relationship has previously been established only for the case of ad-hoc linear spring compliance models and for objects that are immobilized to first-order [18]. Second-order immobility, which relies upon the use of surface curvature effects to reduce the number of fingers needed to immobilize an object, is a new concept. Hence it was necessary to investigate its validity when the practically important effects of compliance are taken into account. We showed that an elastic deformation contact model yields a satisfactory explanation of the forces of restraint generated by curvature effects. This result provides physical justification for applications of second-order mobility theory. We do not indent to imply that second-order effects should always be relied upon in practice. However, there are numerous applications where second-order effects are sufficient, and afford a useful reduction in the complexity of grasp/fixture planning. We sketch below some obvious applications of this work, in order to highlight the particular role that second-order effects may play.

Work Holding: In the companion paper [22] we already considered the use of 2nd-order effects to prove new lower bounds on the number of frictionless fingers necessary to immobilize an object. In this paper we justified these results from a dynamic perspective. These results have obvious uses for *fixture planning.* Previous investigators have analyzed

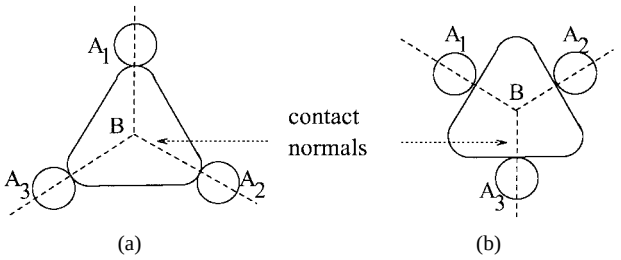

Fig. 8. (a) Maximal three-finger equilibrium grasp (b) minimal three-finger grasp.

the fixture planning problem and have proposed algorithms based on first-order mobility theories (see [2] and [15] for example). Our second-order mobility results suggest that many objects can be immobilized with substantially fewer numbers of fixtures than previously thought possible. In a sequel to this paper [21] (written after this paper was submitted), we indeed establish the new bounds for planar objects. In [12], we also showed by way of analysis and examples that the effective stiffness of grasps that rely upon second-order effects can be comparable to those employing first-order effects. Moreover, it is often true that machining forces are restricted to a subspace or subset of the wrench space. Hence, fixtures need not be uniformly stiff in all directions, and the reduction in number of fixtures afforded by second-order effects may lead to simpler fixture planning algorithms and more useful fixturing arrangements.

Differentiating Between Equilibrium Grasps: Not all equilibrium grasps are alike, and a careful grasp planner should choose the most secure grasps. First, the value of the 2nd-order mobility index, $m^2_{q_0}$, can be used to determine the different degrees of mobility of alternate equilibrium grasps of $\mathcal{B}$ which involve the same number of fingers. As an example, consider the three-finger maximal grasp of Fig. 8(a), and the minimal grasp of Fig. 8(b). Both grasps have the same 1st-order mobility index of $m^1_{q_0} = 1$. However, $m^2_{q_0} = 1$ for the maximal grasp while $m^2_{q_0} = 0$ for the minimal grasp. Since lower index grasps are inherently less mobile, and hence more secure, the minimal grasp is preferred. Similarly, the two-finger grasps seen in Fig. 9(a), (b), and (d) have the same 1st-order mobility index, but different 2nd-order mobility index. Note, however, that our theory cannot distinguish between the grasps of Fig. 9(b) and (c). In a sequel to this paper [13], we consider quality measures which take into account the overall grasp stiffness and can differentiate between these grasps.

Posture planning (planning with force constraints): Consider the problem of planning the motion of a mobile articulated robot in a stationary piecewise rigid environment. Examples are a "snake-like" robot that crawls inside a tunnel while embracing against its sides, or a limbed robot (analogous to a "monkey") that climbs a trussed structure. In all of these examples we are primarily concerned with planning a sequence of "hand-hold" states (analogous to the hand-holds used by rock climbers between dynamically moving states) where the robot mechanism is at a static equilibrium. We call this problem *quasistatic locomotion planning*. On purely kinematic grounds, there is a duality between grasp planning and posture planning. The analysis in this paper is useful for planning quasistatic locomotion, since we can map the mechanism-environment pair to its dual fingers-object pair in the grasp planning problem. The use of second-order effects can be critical in such applications, since it allows for fewer numbers of legs in the mechanism design. This reduction leads to overall system and locomotion planning simplicity.

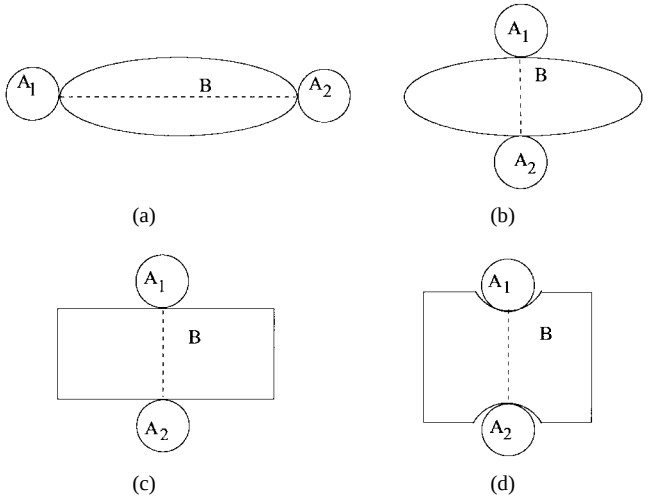

Fig. 9. The 2nd-order mobility index of 1st-order equivalent equilibrium grasps. (a) 2nd-order mobility 2, (b) 2nd-order mobility 1, (c) 2nd-order mobility 1, and (d) 2nd-order mobility 0.

APPENDIX
DETAILS OF THE ELASTIC CONTACT MODEL

We begin with a proposition which gives a formula for the wrench generated by the elastic contact force $F_i(x_i)$. We need the following two lemmas.

Lemma A.1 [20]: Let $q_0 = (d_0, \theta_0)$ and let $\mathcal{B}(q_0)$ overlap $\mathcal{A}_i$, such that x_i and y_i are the endpoints of the overlap segment. If $o_i(d, \theta_0)$ is differentiable at d_0 and $\frac{\partial}{\partial d}|_{d=d_0}$ is nonzero, then $\frac{\partial}{\partial d}|_{d=d_0} o_i(d, \theta_0) = -\frac{y_i - x_i}{\|y_i - x_i\|}$.

In the following, $X_{r_i}(q)$ is the rigid-body transformation which maps the ith contact point from $\mathcal{B}$'s body coordinates, r_i, to its world coordinates, x_i.

Lemma A.2 [20]: If $\mathcal{A}_i$ is stationary, $\dot{o}_i$ is the projection of $\dot{X}_{r_i}$ along the overlap segment $\overline{x_i y_i}$. That is, $\dot{o}_i = -\hat{N}(x_i) \cdot \dot{X}_{r_i}$.

Proposition 2.3: Let $\mathcal{A}_i$ be stationary and let $\mathcal{B}(q)$ have overlap $o_i(q) > 0$ with $\mathcal{A}_i$. Any interbody force $F_i(x_i)$ acting on $\mathcal{B}$ along the the overlap segment $\overline{x_i y_i}$ into $\mathcal{B}$ gives a **wrench** of the form: $w(q, F_i) = -\|F_i\| \nabla o_i(q)$.

Proof: According to Theorem 1 of [22], the force $F_i(x_i)$ gives rise to a wrench $w(q, F_i) = [DX_{r_i}(q)]^T F_i(x_i)$. We need only to consider points q in the interior of $\mathcal{CA}_i$, since $w(q, F_i)$ vanishes at all other configuration points q. First we show that $w(q, F_i)$ is collinear with $\nabla o_i(q)$. (We treat the covector $w(q, F_i)$ and the tangent vector $\nabla o_i(q)$ as vectors in $I\!R^m$.) Thus we have to show that $w(q, F_i) \cdot \dot{q} = 0$ for all $\dot{q}$ based at q, such that $\nabla o_i(q) \cdot \dot{q} = 0$.

By the chain rule, $\frac{d}{dt}o_i(q(t)) = \nabla o_i(q)\cdot\dot{q}$. But $\dot{o}_i = -\hat{N}(x_i)\cdot\dot{X}_{r_i}$ according to Lemma A.2. Hence $\hat{N}(x_i)\cdot\dot{X}_{r_i} = 0$ for all $\dot{q}$ such that $\nabla o_i(q)\cdot\dot{q} = 0$. This, together with the *virtual work principal*, imply that $w(q,F_i)\cdot\dot{q} = \|F_i\|(\hat{N}(x_i)\cdot\dot{X}_{r_i}) = 0$. Thus $w(q,F_i)$ is collinear with $\nabla o_i(q)$, i.e., $w(q,F_i) = \lambda\nabla o_i(q)$ for some scalar λ. To complete the proof, we must show that $\lambda = -\|F_i\|$. Using Lemma A.1 and Lemma 2.1, at points where o_i is differentiable (which is the case in some open neighborhood about $\mathcal{S}_i$), $\frac{\partial}{\partial d}o_i(d,\theta) = -(y_i - x_i)/\|y_i - x_i\| = -\hat{N}(x_i)$. On the other hand, it can be verified by computing the derivative of $X_{r_i}(q)$ that $w(q,F_i) = DX_{r_i}(q)^T F_i(x_i) = \left(\begin{smallmatrix} F_i(x_i) \\ Rr_i\times F_i(x_i)\end{smallmatrix}\right)$. Thus we have that $\left(\begin{smallmatrix} F_i(x_i) \\ Rr_i\times F_i(x_i)\end{smallmatrix}\right) = \lambda\left(\begin{smallmatrix} -\hat{N}(x_i) \\ \frac{\partial}{\partial\theta}o_i(d,\theta)\end{smallmatrix}\right)$. But $F_i = \|F_i\|\hat{N}(x_i)$ when F_i is pushing into $\mathcal{B}$, hence $\lambda = -\|F_i\|$. □

The following lemma and its corollary ensure that while o_i is nonsmooth, o_i^2 is differentiable.

Lemma A.3: Given a smooth real-valued function $f(x)$, the function $g(x) = (\max\{f(x),0\})^2$ is **differentiable** with Lipschitz continuous derivative, and its derivative is

$$\nabla g(x) = 2\max\{f(x),0\}\nabla f(x).$$

Proof: Using the chain rule

$$\nabla g(x) = 2\max\{f(x),0\}\nabla(\max\{f(x),0\}). \tag{11}$$

It can be verified that $\max\{f(x),0\}$ can be written in the following equivalent form:

$$\max\{f(x),0\} = \frac{1}{2}(f(x) + |f(x)|) = \frac{1}{2}(f(x) + \sqrt{f^2(x)})$$

where we have used the identity $|f(x)| = \sqrt{f^2(x)}$. Substituting this identity into (11) and taking the derivative gives $\nabla g(x) = \max\{f(x),0\}(\nabla f(x) + \frac{f(x)}{\sqrt{f^2(x)}}\nabla f(x))$. Propagating $\max\{f(x),0\}$ into the parentheses yields the result. As for the Lipschitz continuity of $\nabla g(x)$ see, e.g., [3, p. 47].

In our case, $o_i = \max\{\tilde{o}_i,0\}$, where $\tilde{o}_i$ is the following *signed* overlap function:

$$\tilde{o}_i(d,\theta) \triangleq \begin{cases} \mathsf{dst}(d,\mathcal{S}_i|_\theta), & \text{if } q=(d,\theta) \text{ is inside } \mathcal{CA}_i \\ -\mathsf{dst}(d,\mathcal{S}_i|_\theta), & \text{if } q=(d,\theta) \text{ is outside } \mathcal{CA}_i. \end{cases}$$

The signed overlap function $\tilde{o}_i$ is identical to o_i in the interior of $\mathcal{CA}_i$, zero on $\mathcal{S}_i$, and strictly negative outside of $\mathcal{CA}_i$. If $\mathcal{S}_i$ is smooth, as in our case, $\tilde{o}_i$ is smooth in a neighborhood of $\mathcal{S}_i$. We can thus state the corresponding result for o_i.

Corollary A.4: $\frac{1}{2}o_i^2$ is **differentiable** with Lipschitz continuous derivative, and its derivative is

$$\nabla\left(\frac{1}{2}o_i^2\right) = \begin{cases} o_i\nabla o_i & \text{if } o_i > 0 \\ 0 & \text{if } o_i = 0. \end{cases} \tag{12}$$

ACKNOWLEDGMENT

The authors would like to thank Dr. M. Mason for calling their attention to the ellipse paradox.

REFERENCES

[1] D. Baraff, "Issues in computing contact forces for nonpenetrating rigid bodies," *Algorithmica*, vol. 10, pp. 292–352, Oct. 1993.
[2] R. C. Brost and K. Y. Goldberg, "A complete algorithm for synthesizing modular fixtures for polygonal parts," in *Proc. IEEE Int. Conf. Robot. Automat.*, San Diego, CA, May 1994, pp. 535–542.
[3] F. H. Clarke, *Optimization and Nonsmooth Analysis*. Philadelphia, PA: SIAM, 1990.
[4] M. R. Cutkosky and I. Kao, "Computing and controlling the compliance of a robotic hand," *IEEE Trans. Robot. Automat.*, vol. 5, pp. 151–165, Apr. 1989.
[5] F. Featherstone, "Dynamics of rigid body systems with multiple concurrent contacts," in *Robotics Research: The Third International Symposium*, O. D. Faugeras and G. Giralt, Eds. Cambridge, MA: MIT Press, 1986, pp. 189–196.
[6] Fujita and Hattori, "Periodic vibration and impact characteristics of a nonlinear system with collision," *Bull. JSME*, vol. 177, pp. 409–417, 1980.
[7] A. Gesley, "From cad/cam to simulation: Automatic model generation for mechanical devices," in *Knowledge-Based Simulation: Methods and Applications*, P. Fishwick and R. Modjeski, Eds. New York: Springer-Verlag, 1989.
[8] H. Hanafusa and H. Asada, "Stable prehension by a robot hand with elastic fingers" in *Proc. 7th Int. Symp. Ind. Robots*, 1977, pp. 384–389.
[9] H. Hertz, "On the contact of elastic solids," in *Miscellaneous Papers by H. Hertz (1882)*. London, U.K.: Macmillan, 1896.
[10] W. S. Howard and V. Kumar, "On the stability of grasped objects," *IEEE Trans. Robot. Automat.*, vol. 12, pp. 904–917, Dec. 1996.
[11] D. E. Koditschek, "The application of total energy as a Lyapunov function for mechanical control systems," in *Control Theory and Multibody Systems, AMS Series in Contemporary Mathematics*, J. Marsden, Krishnaprasad, and J. Simo, Eds. Providence, RI: 1989, vol. 97, pp. 131–158.
[12] Q. Lin, J. W. Burdick, and E. Rimon, "Computation and analysis of compliance in grasping and fixturing," in *Proc. IEEE Int. Conf. Robot. Automat.*, Albuquerque, NM, May 1997.
[13] Q. Lin, J. W. Burdick, and E. Rimon, "A quality measure for compliant grasps," in *IEEE Int. Conf. Robot. Automat.*, Albuquerque, NM, May 1997.
[14] M. Mason, personal communication, May 1993.
[15] B. Mishra, "Workholding," in *Proc. IEEE/RSJ Int. Conf. Intell. Robots Syst.*, 1991, pp. 53–57.
[16] D. J. Montana, "The kinematics of contact with compliance," in *IEEE Int. Conf. Robot. Automat.*, 1988, pp. 770–774.
[17] D. J. Montana, "Contact stability for two-fingered grasps," *IEEE Trans. Robot. Automat.*, vol. 8, pp. 421–230, Aug. 1992.
[18] V.-D. Nguyen, "Constructing force-closure grasps," *Int. J. Robot. Res.*, vol. 7, no. 3, pp. 3–16, June 1988.
[19] J. Ponce, "On planning immobilizing fixtures for 3d polyhedral parts," in *Proc. IEEE Int. Conf. Robot. Automat.*, Minneapolis, MN, May 1996, pp. 821–827.
[20] E. Rimon and J. W. Burdick, "Curvature effects of bodies in contact: Their impact on mobility and their forces of restraint," Tech. Rep. RMS-93-01, Dept. of Mech. Eng., California Inst. Technol., Pasadena, Sept. 1993.
[21] ———, "New bounds on the number of frictionless fingers required to immobilize planar objects," *J. Robot. Syst.*, vol. 12, no. 6, pp. 433–451, June 1995.
[22] ———, "Mobility of bodies in contact—I; A 2nd-order mobility index for multiple-finger grasps," *IEEE Trans. Robot. Automat.*, this issue, p. 696–708.
[23] P. R. Sinha and J. M. Abel, "A contact stress model for multifinger grasps of rough objects," *IEEE Trans. Robot. Automat.*, vol. 8, pp. 7–22, Feb. 1992.
[24] Sir W. Thompson and P. G. Tait, *Treatise on Natural Philosophy*. Cambridge, U.K.: Univ. Cambridge Press, 1886.

Elon Rimon, for a biography, see this issue, p. 708.

Joel W. Burdick, for a biography, see this issue, p. 708.